Engineering Structures 253 (2022) 113757

Contents lists available at ScienceDirect

Engineering Structures

journal homepage: www.elsevier.com/locate/engstruct

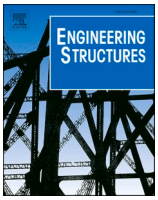

Improved seismic response of light-frame-timber panels with cement-particle-board sheathing of various thicknesses and different configurations of fasteners

Meta Kržan [a,*], Tomaž Pazlar [a], Boštjan Ber [b]

[a] ZAG Ljubljana (Slovenian National Building and Civil Engineering Institute), Ljubljana, Slovenia
[b] Jelovica hiše, Slovenia

ARTICLE INFO

Keywords:
Light-frame timber panels
Cement-particle board sheathing
Cyclic shear tests
Sheathing-to-timber connection
Asymmetrical panel
Staple spacing distance
EN 1995–1-1

ABSTRACT

Due to their comparable fire characteristics and surface preparation, light-frame timber panels using cement-particle boards (CPB) as a sheathing material present a potential alternative to gypsum-fibre boards. An experimental campaign was conducted to evaluate the behaviour of CPB light-frame-timber panels under in-plane lateral loading. Monotonic and cyclic in-plane shear tests were conducted on full-size panels, following preceding tests on the stapled sheathing-to-timber connections used in the panels. The influence of the boards' thickness and staple geometry on the response of connections and panels was studied, also on panels with an asymmetrical CPB layout, which proved not to have a negative influence on the panels' lateral load-bearing capacity. Furthermore, in order to improve the seismic response, panels, which had almost twice the number of staples compared to the basic panel, were tested; one variation with two rows of staples, and the other with the staples spaced closer together, such that the spacing distance was halved. The tests revealed a significant, though not proportional, increase in lateral resistance in the strengthened panels. Fastening the CPB with two rows of staples proved the better option, since subsequent failure of the CPB along the connections, as opposed to ductile failure of the staples in the basic panels, proved not to reduce the panels' deformation capacity. The paper also compares the test results of the connections and panels to analytical results according to Eurocode 5 (EC5), the European code provision for the design of timber structures.

1. Introduction

1.1. Motivation

Despite the exponential increase in the use of cross-laminated-timber (CLT) for structural purposes, light-framed timber structures remain the most widespread timber-based structural system worldwide. Light-frame timber panels (LFTP) have a number of advantages over CLT panels, including: i) a substantial reduction in the consumption of timber; ii) the ability to place insulation and technical installations inside the panels, reducing the wall thickness and number of cut-outs required, respectively; iii) improved fire resistance, given the choice of available sheathing materials. Due to the reasons mentioned, and the fact that sustainability and construction speed are becoming increasingly important, midrise light-frame timber structures are also becoming more common these days.

With higher and more complex structures, however, the seismic loading also increases, and in seismic regions this often becomes the most critical loading in the design of structures. There is thus a need for an improved understanding of the behaviour of panels and input parameters required for seismic design, as well as a need to improve their performance.

LFTP are constructed of a timber frame, where the vertical framing members (studs) provide resistance to vertical loads, while the lateral resistance and stiffness of the panels are provided through sheathing. The sheathing boards, made from various materials (most commonly gypsum-fibre boards (GFB) and oriented-strand boards (OSB)), are fastened to the timber frame by various types of mechanical dowel, according to the type of sheathing used (usually nails or staples). Although various parameters, such as the panel geometry aspect ratio, anchoring of the panels, level of vertical load and type of sheathing, all influence the lateral behaviour of the panels, the sheathing-to-timber

* Corresponding author.
E-mail addresses: meta.krzan@zag.si (M. Kržan), tomaz.pazlar@zag.si (T. Pazlar), bostjan.ber@jelovica.si (B. Ber).

https://doi.org/10.1016/j.engstruct.2021.113757
Received 29 July 2021; Received in revised form 10 November 2021; Accepted 7 December 2021
Available online 27 December 2021
0141-0296/© 2021 The Authors. Published by Elsevier Ltd. This is an open access article under the CC BY license (http://creativecommons.org/licenses/by/4.0/).

connections are also crucial for understanding and predicting the lateral load-bearing, stiffness and deformation capacity of LFTP [1,2]. Connections should allow energy dissipation through a number of plastic deformations in the connectors, and ductile failure of the panels, in order to obtain a behaviour factor favourable for the seismic design of LFTP structures.

1.2. Subject of research

The goal of the experimental campaign presented was to comprehensively study the seismic behaviour of LFTP with cement-particle boards (CPB) used as the sheathing material. In contrast to other sheathing materials, no studies can be found for the seismic behaviour of LFTP or sheathing-to-timber connections using CPB. This is likely because only a few producers of prefabricated light timber structures use such panels, despite the fact that they present a good alternative to GFB, with comparable fire characteristics and panel plastering and rendering, which are decisive reasons for the increased use of GFB in comparison to other types of sheathing material.

The research goal was to evaluate the behaviour of panels already used in construction, but the study also aimed to investigate potential ways to increase the lateral resistance of panels and improve their seismic response. To analyse the seismic behaviour of panels used in practice, panels of different CPB thickness were evaluated. Shear tests were also conducted on an asymmetrical variation of the panel, with CPB of different thicknesses on either side of the panel, in order to confirm whether a minimum of 50% reduction in lateral load-bearing capacity, as suggested in the current European code provision for design of timber structures, EC5 (EN 1995–1-1, [3]), is indeed required for the panels investigated.

Prior to carrying out monotonic and cyclic shear tests on full-size panels, experimental tests of CPB-to-timber connections with metal staples, were conducted on smaller specimens. The tests were conducted for three main reasons: i) to determine whether the response of the connectors used, and their configuration, resulted in a favourable failure mechanism at the component level of the connections; ii) to explore potential options to strengthen the panels through the systematic study of different connector configurations, by reducing the spacing distance between staples, and by fastening the CPB with two rows of staples as opposed to one, and; iii) to compare the experimentally obtained results to those obtained analytically according to EC5.

Following testing of the sheathing-to-timber connections, in addition to the panels used in practice, two panel variations with higher number of sheathing-to-timber connections were also tested under cyclic lateral loading. Experimental tests of panels with such design of sheathing-to-timber connections have not yet been conducted. To analyse and compare the results, the results of panel and connection tests were evaluated in terms of various parameters important for seismic behaviour, such as resistance and deformation capacity, ductility and energy dissipation. Finally, both sets of results were compared to analytical predictions according to EC5, in order to establish whether the estimations, which are used in practice for the design, are for the tested panels conservative (or not), and consistent, for the type of sheathing used.

1.3. Brief overview of the literature

An extensive experimental campaign on sheathing-to-timber connections, including various sheathing materials, sheathing thickness and connectors, was conducted by Fonseca et al within the CUREE - Caltech Woodframe Project [4], by Sartori and Tomasi [5] and by Seim et al [6]. The latter two studies showed that, when using GFB as a sheathing material, the load-bearing capacity and stiffness of connections was similar to an OSB system, but ductility was significantly lower. In [5], the GFB behaved in a brittle manner, and also exhibited a lower dissipation of energy, while in [6], similar values of equivalent viscous damping were obtained for the two different sheathing materials, establishing that panels need to be tested in order to confirm their behaviour under lateral loads. Furthermore, it was established in [5] that the analytical results for the tested GFB-staple connections underestimate the load-bearing capacity by up to 55%, with European yield model (EYM) in EC5 [3] providing the best estimation (the smallest discrepancy compared to experimental values). On the other hand, the code corresponded better to the results of nail-OSB connections. The study conducted by Verdret et al [7], which compared the OSB-to-timber connections with staples and nails, proved that experimental results compared well to the analytical results according to EC5 for both types of connection. For OSB-to-timber connections with nails, Seim et al [8] found that the EYM is more conservative when the thickness of the OSB sheathing is 10 mm instead of 18 mm.

On the contrary to cyclic tests on sheathing-to-timber connections, numerous experimental as well as numerical studies can be found regarding the behaviour of LFTP under lateral loading, with various research interests; a comprehensive overview of the various studies until 2004 was presented by van de Lindt [9], while a more recent review can be found in study of the Di Gangi et al [10], which also provides an exhaustive overview of numerical and analytical approaches towards the analysis of LFTP.

Of particular interest with regard to the present research are the studies that investigated the influence of the sheathing material on the behaviour of LFTP. In [6], the ductility and equivalent viscous damping obtained in cyclic tests were similar in double sheathed GFB and OSB panels, but smaller in single sheathed GFB panels than in single sheathed OSB panels. An asymmetrical panel, with OSB on one side and GFB on the other, was monotonically tested by Sartori et al [11], with the results revealing a significant decrease in strength due to brittle failure of the GFB. The influence of various structural detailing on the lateral behaviour of LFTP was studied by Bagheri and Doudak [12], who found that, while the diameter and spacing of nails significantly affect the panels' load-bearing capacity, this effect is not linear. Within the literature, various attempts have been made to increase the lateral load-bearing capacity and stiffness of LFTP, through, for example, the use of additional GFB [13], or the use of strong anchorages [14]. A very high lateral load-bearing capacity with good deformation capacity was obtained in a double-sheathed GFB panel, where the gap between the GFB had been adhesively bonded [15]. In seismic design, not only the lateral load-load bearing capacity is important, but also the capacity for high deformation and ductility through predetermined mechanisms for energy dissipation. In the present paper, the influence of varying the number and configuration of sheathing-to-timber connections is studied, with a view to improving the lateral response.

According to the state-of-the art review by Jayamon et al [16] regarding the damping of timber-frame walls, the spacing distance between sheathing-to-timber-connections also influences the damping characteristics of timber shear walls. It was observed that smaller spacing between fasteners leads to increased damping due to larger internal frictional forces, mobilized by slippage of the fasteners. Experimental tests conducted by Steiger et al [17] proved, that the friction coefficients between adjacent OSB panels and OSB panels versus glued laminated timber are decreasing with increasing cumulative displacements due to grinding of the surface. Di Gangi et al [10], however, who conducted an extensive numerical study regarding the optimisation of performance and cost in LFTP, observed that, as opposed to resistance, an almost negligible increment in equivalent viscous damping is obtained by increasing the spacing between fasteners (at comparable

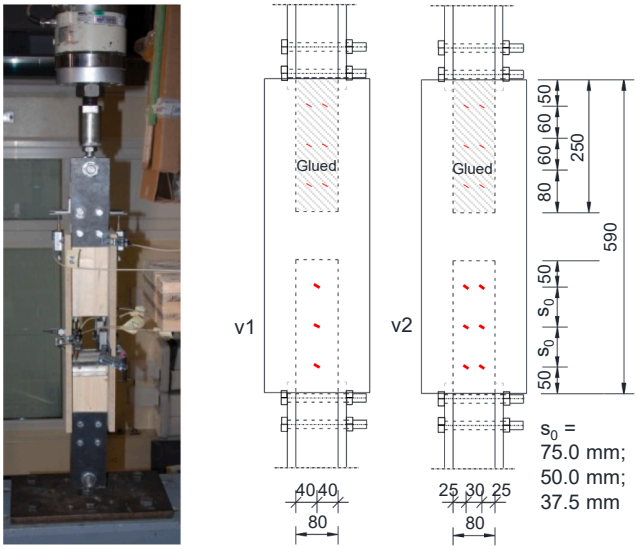

Fig. 1. a. Test setup for sheathing-to-timber connections tests; b. Geometry of the specimens with one (v1) and two (v2) rows of staples.

drifts).

2. Materials and methods

Since the idea of the tests was to better understand the behaviour of wall panels already used in construction, small specimens of three types, designed to test the connections as well as panels of different thicknesses, were tested: i) specimens with 12 mm CPB on both sides (labelled B12-12); ii) specimens with 16 mm CPB on both sides (labelled B16-16) and iii) specimens with 12 mm CPB on one side and 16 mm on the other (labelled B12-16). The B12-12, B16-16 and B12-16 labels are used throughout the paper to refer to both connection and panel specimens.

2.1. Materials

Both the small specimens and the wall panels were constructed from the same materials. All framing members of the panels, as well as the small specimens, were constructed from GL 24 h timber. The characteristic mechanical characteristics of the CPB, as provided by the producer, are as follows: bending strength $f_{m,k} = 9.0$ MPa, tensile strength $f_{t,k} = 2.5$ MPa, shear strength $f_{v,k} = 6.5$ MPa, compressive strength $f_{c,k} = 11.5$ MPa and elasticity modulus $E_{m,mean} = 4500$ MPa. The CPB were fixed to the timber elements with metal staples with a staple wire tensile strength of $f_{u,k} = 900$ MPa and a thermo-adhesive layer applied to the legs [18]. The staples were inserted into the timber with the staple crown at an angle 30° with respect to the direction of the timber grain. A staple size of 1.53 × 11.25 × 45 mm was used for the 12 mm CPB (B12) and 2.0 × 11.76 × 50 mm for the 16 mm (B16) CPB.

2.2. Experimental tests of sheathing-to-timber connections

To evaluate the load-bearing capacity and behaviour of the sheathing-to-timber connections, and to determine whether the spacing between the staples in the panels could be reduced, small specimens replicating part of the timber frame panels were designed and constructed, with CPB on both sides fastened to the timber elements by metal staples (Fig. 1a).

The recommended longitudinal distance between fasteners ranges between 100 and 300 mm for 12 mm and 16 mm thick CPB, according to various producers. This is more than the recommendations according to EN 1995–1-1, which gives a minimal longitudinal spacing distance of 15.3 mm and 20 mm for the staple diameters used in B12 and B16, respectively, regardless of the sheathing material used. Three or six (two rows of three) staples, at different, equidistant, longitudinal spacing s_0 (75, 50 or 37.5 mm), were therefore used to fasten the board on each side of the specimen (Fig. 1b). Additionally, in order to ensure the failure of the specimen in the connections being investigated, the other side of the board was attached to the timber with adhesive. Due to an overestimation of CPB tensile strength, and an underestimation of the load-bearing capacity of the connections, tensile failure of the CPB occurred in some specimens, so some additional specimens with an increased CPB width (400 mm instead of 200 mm) were also tested. The various test

Table 1
Testing program for sheathing-to-timber connections.

Staple distance	No. of staples on one side	Conducted connections tests				
s_0 (mm)		(Specimen label; Sheathing thickness (mm) × width (mm))				
		B12-12; 12 × 200 (2x)	B16-16; 16 × 200 (2x)	*B16-16; 16 × 400 (2x)	B12-16; 16 × 200, 12 × 200	*B12-16; 16 × 400, 12 × 400
37.5	1 × 3	M, 2 × C	M, C	M, 2 × C	M, C	M, C
50.0		M, 2 × C	M, C	M, 2 × C	M, C	M, 2 × C
75.0	(v1)	M, 2 × C	M, C	M, 2 × C	M, C	M, 2 × C
37.5	2 × 3	M, 2 × C	M, 2 × C	/	M, C	/
50.0		M, 2 × C	M, C	/	M, C	/
75.0	(v2)	M, 2 × C	M, C	/	M, C	/

Note: Labels v1 and v2 denote specimens with 1 and 2 rows of staples, respectively, M and C denote monotonic and cyclic tests, respectively, * denotes specimens with a larger sheathing width (400 mm instead of 200 mm).

Table 2
Wall panel testing program.

Test panel	Loading	Sheathing	Staples: φ / crown / legs	Staples: distance s_0, no. of rows	Anchoring hold-downs
B16-16/75x1	M, 2xC	2 × CPB 16 mm	2.0 / 11.76 / 50 mm	75.0 mm, 1 row	2 × 2 HTT22
B12-12/75x1	M, 2xC	2 × CPB 12 mm	1.53 / 11.25 / 45 mm	75.0 mm, 1 row	2 × 2 HTT22
B12-16/75x1	M, 2xC	CPB 12 mm, CPB 16 mm	1.53 / 11.25 / 45 mm, 2.0 / 11.76 / 50 mm	75.0 mm, 1 row	M: 2 × custom hold-downs, C: 2 × 2 HTT22
B12-12/75x2	2xC	2 × CPB 12 mm	1.53 / 11.25 / 45 mm	75.0 mm, 1 row	2 × WHT740 + WHTBS130
B12-12/37.5x1	2xC	2 × CPB 12 mm	1.53 / 11.25 / 45 mm	37.5 mm, 2 rows	2 × WHT740 + WHTBS130

Note: M and C denote the monotonic and cyclic tests conducted.

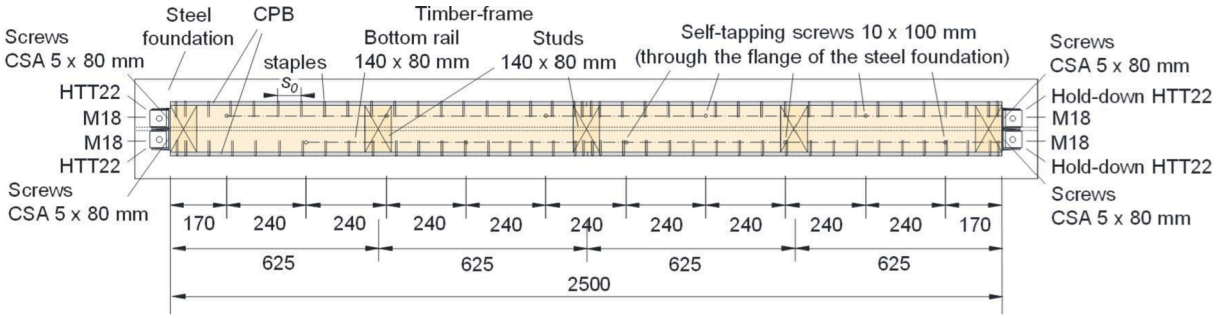

Fig. 2. Cross section of the basic panel with CPB sheathing, anchored to the steel foundation.

specimens and the tests conducted are summarized in Table 1.

One monotonic and one or two cyclic tests were conducted for each specimen. The specimens were fixed in the test setup (Fig. 1a), with free rotation through thick steel plates and four M10 screws on each side. A servo-hydraulic actuator with a capacity of 160 kN was used for the bi-directional loading. The monotonic tests served to determine the loading protocol for the cyclic tests, which were conducted according to ISO 16670:2003 [19], with a subsequent increase in the amplitude displacement based on the average results from the monotonic tests. In the monotonic tests loading was controlled through displacement of the servo-hydraulic actuator, while in cyclic tests it was controlled by the average displacement between the CPB and the timber on the side of the specimen being investigated, measured with four LVDT (two on each CPB, Fig. 1). The loading rate for both monotonic and cyclic tests was 0.1 mm/s.

2.3. Experimental tests of full-scale wall elements

Five variations of panels were tested. Three basic variations studied the influence of board thickness; B12-B12, B16-16 and the asymmetrical B12-16 panel, using the same sheathing-to-timber connection details as is currently used in practice. The influence of increasing the number of fasteners on the behaviour of the panels was further studied on two variations of the B12-12 panel. In these tests the number of staples was increased, with the staples arranged in two different configurations. The various details of the panels tested are summarised in Table 2.

The size of the panels tested was 2.50 × 2.64 m (length × height), while the width varied according to the thickness of the CPB. For the basic panels the timber frames were constructed of five studs (140/80 mm) at equidistant spacing (625 mm), and a bottom rail of dimensions 140/80 mm (Fig. 2). The cross section of the upper rail was 140/160

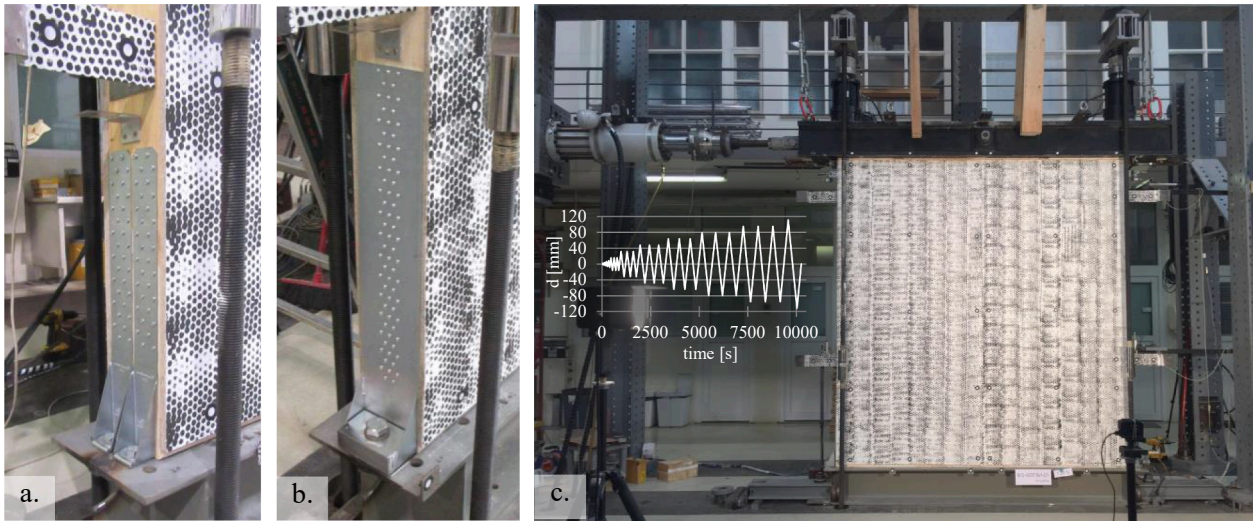

Fig. 3. a. Standard hold-downs to anchor weaker panels; b. Stronger hold-down to anchor the strengthened panels; c. Test setup for shear tests on the wall panels with cyclic tests loading time history.

mm. Prior to sheathing, the frame was constructed by joining the studs and rails with corrugated staples (two per joint, no other mechanical fasteners were used in the frame construction). The covering consisted of two CPB sheathing panels (1.25 × 2.5 m) attached to either side of the frame with staples. In all the basic panels the staples were spaced at a distance of 75 mm along the outside edge of each panel, and at a distance of 150 mm along the interior studs. All basic specimens with the CPB fastened in this way are denoted by /75x1. For panels B12-12 with more staples on the outside edge of the CPB, the sheathing was either fixed to the timber with staples spaced at half the distance, i.e. 37.5 mm apart (labelled as B12-12/37.5x1), or with the staples placed in two rows along the edge, spaced 75 mm apart (denoted B12-12/75x2). In the latter case the bottom rail of the frame was thicker (140/160 mm), and two studs (2 × 140/80 mm) were used instead of one in the middle and on each side so that two rows of staples could be used to fasten the boards while maintaining a sufficient distance between the staples, as well as between the staples and the edge of the timber. The distance between the two rows was 20 mm, with the staples staggered in both rows.

In all specimens except the B12-16/75x1/M, shear sliding of the panels was prevented by 10 STS 10 × 100 mm screws [20]; in the B12-16/75x1/M specimen it was prevented by four AE116 [21] angle brackets equally spaced apart. The anchoring for the tension forces was chosen according to the results of the first panel test (B12-16/75x1/M), for which a stronger custom made hold-down was used to prevent the failure of the panel in the anchoring area. For all the other panels, commercially available hold-downs (as used in practice) were used with the grade of overdesign predefined by the 140 mm thickness of the studs (overdesign smaller than 2.15 as recommended by Schick and Seim [22], though). The geometry allowed for two commercial hold-downs for the basic panels (Fig. 3a, [23]) and one stronger hold-down for the strengthened panels (Fig. 3b, [24]) to be fixed on each side.

For each type of the basic specimens, 1 monotonic and 2 cyclic racking tests were conducted, while 2 cyclic tests were carried out for each type of strengthened panel. Vertical and horizontal loading were applied through a steel beam placed over the top rail (Fig. 3c). Vertical loading of 25 kN/m was applied with two hydraulic actuators placed on the steel beam, and kept constant during the shear loading. Horizontal loading was induced by controlling the increase in lateral displacement at the top of the panel. The time history loading protocol for the cyclic tests was defined according to ISO 16670: 2003 [19] based on the results from the monotonic tests (performed according to EN 594: 2011 [25]). Within the same amplitude displacement loading cycles the loading rate was constant, in the range 0.1–0.5 mm/s.

The displacements of panels during the tests were measured with 6 LVDTs and an optical measuring system, which measured displacements of the CPB, the side studs of the panels, and the base and top steel beams.

3. Results

3.1. Tests of sheathing-to-timber connections

The ductile failure mechanism of both B12 and B16 connections occurred in both monotonic and cyclic tests. The failure mechanism of plastic deformations of the staples, and withdrawal of the staples from the timber, occurred in the cyclic tests of all B12-B12, B12-16 and B16-16 specimens with one row of staples, as shown in Fig. 4 (a and b). In the softening (post-peak) phase of the tests, breakage of the staples also sometimes occurred (Fig. 4c). The asymmetry of the B12-B16 specimens proved not to have a negative influence on the results. Due to tensile failure of the CPB, failure of the connections was not achieved in any of the B16 specimens in the monotonic tests, nor in the B16 specimens with two rows of staples in the cyclic tests (Fig. 4d). In monotonic tests of the B16-16 and B12-16 specimens with one row of staples and a greater CPB width, however, the ductile failure mechanism of the connections previously described also occurred (Fig. 4e).

The distance between staples proved not to influence the failure mechanism; a shear crack in the CPB was initiated on one side of the sample only in the monotonic test (not in the cyclic tests) of the B16-16 specimen with a staple spacing distance of 37.5 mm (Fig. 4f). A typical hysteresis force – lateral displacement curve obtained, together with backbone envelopes of hysteresis curves for all three types of specimens with one row of staples, are presented in Fig. 5a.

To compare the results of specimens with different numbers of staples, however, the lateral load – displacement curves obtained from tests on the symmetrical specimens (B12-12 and B16-16) were normalised per single staple; Fig. 5b shows the normalised results of monotonic tests (per single staple) on samples with one row of staples, while Fig. 6a and 6b show the normalised results of cyclic tests on specimens with one and two rows of staples, respectively. In contrast to hysteresis backbone envelopes in Fig. 5a, where maximum forces obtained are presented for all displacements in order to show the strength degradation with repeating loading cycles, the hysteresis envelopes in Fig. 6 present the maximum forces in amplitude displacements of the first loading cycles.

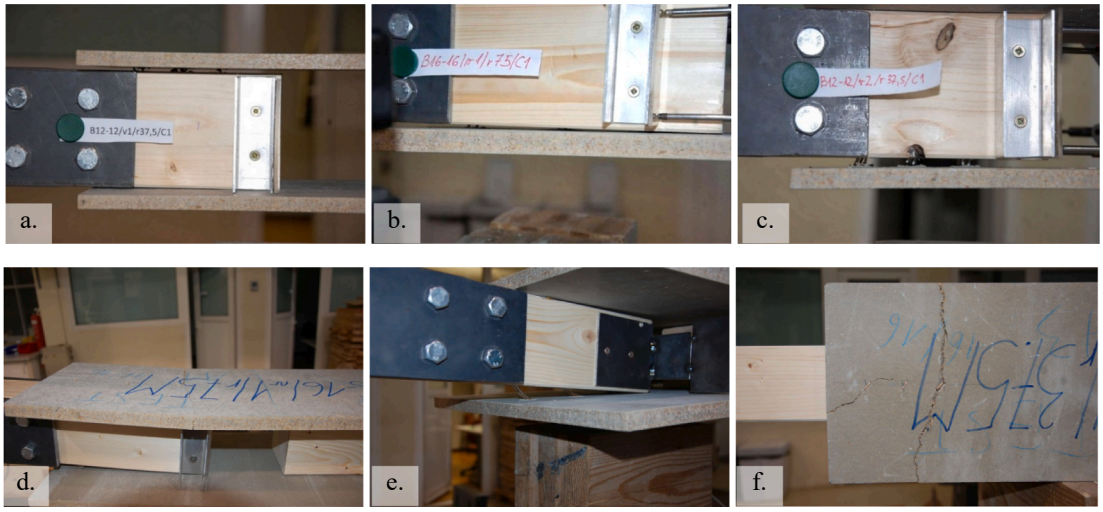

Fig. 4. Typical ductile failure mechanism of the connections with plastic deformations and withdrawal of the staples following the cyclic testing of specimens: a. B12-12; b. B16-16; c. Failure of the staples in the softening phase of loading; d. Tensile failure of the CPB in the monotonic tests on B16-16; e. Ductile failure of the B16 connections under monotonic testing of the specimen with a greater CPB width; f. Shear crack in the B16/v1/r37.5/M specimen.

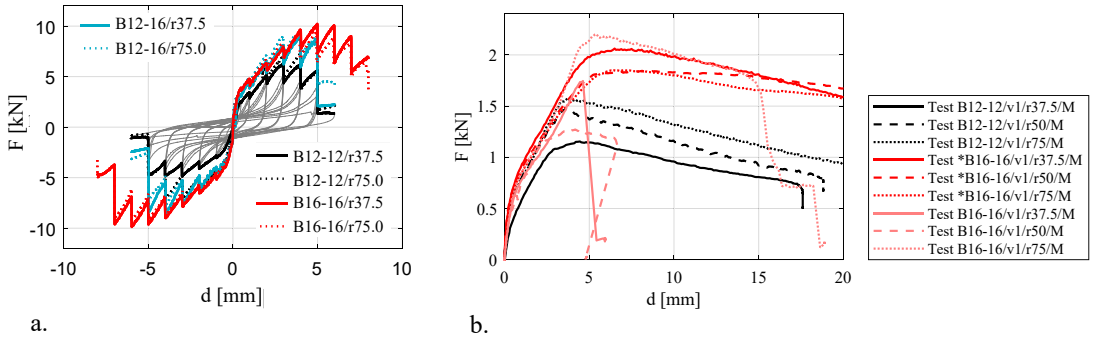

Fig. 5. a. Typical load–displacement hysteresis curve and backbone hysteresis envelope curves for cyclic tests on specimens with one row of staples; b. Load-displacement curves for monotonic tests (per staple) on B12-12 and B16-16 specimens with one row of staples.

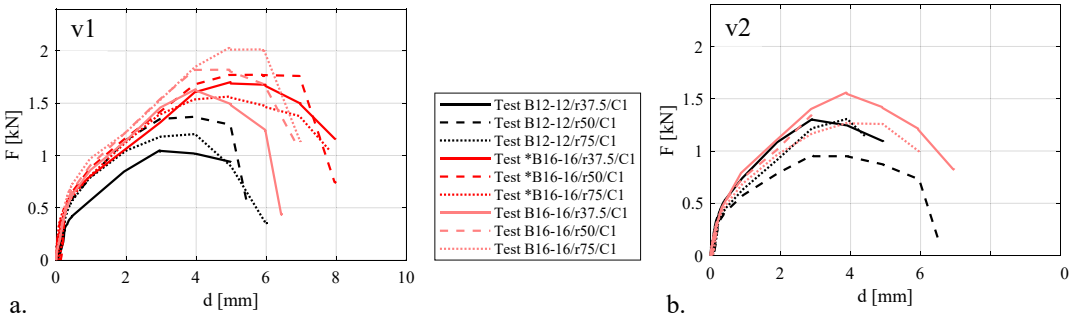

Fig. 6. Load - displacement hysteresis envelope curves (per staple) obtained from cyclic tests on B12-12 and B16-16 specimens with either one (v1) or two (v2) rows of staples.

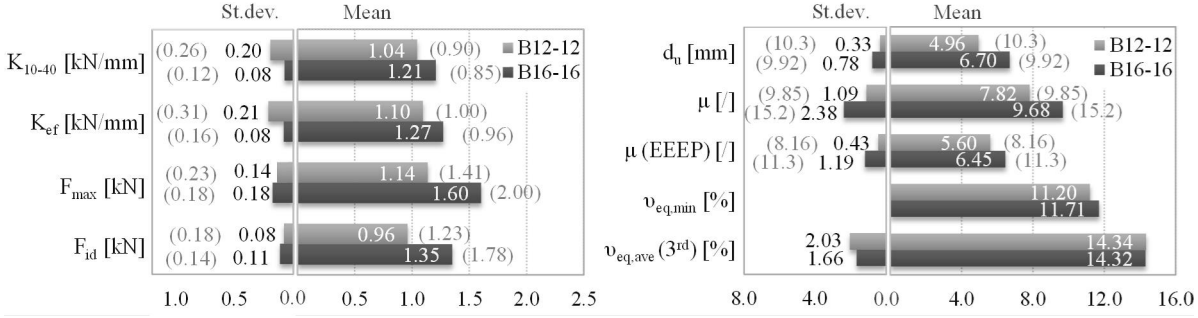

Fig. 7. Average test results of cyclic and monotonic (in brackets) tests per single staple for the two types of connection (from specimens B12-12 and B16-16) with standard deviation (St.dev.).

Since no consistent influence of spacing distance on the lateral load-bearing capacity was found in the cyclic tests, normalised average results for both types of connection are depicted in Fig. 7 for both the cyclic and monotonic tests (considering specimens with all spacing distances and tests where the connection failure was critical). Besides the maximum resistance, F_{max}, and elastic stiffness, $K_{10\text{-}40}$ (i.e. secant stiffness at 10% and 40% F_{max}), the results of idealised bi-linear curves are also presented (Fig. 7). The effective stiffness of the bi-linear curve K_{ef} was evaluated according to EN 12512 [26] using yield slip d_y and corresponding load F_y (as F_y/d_y, see Fig. 8), while the idealised load-bearing capacity F_{id} and elastic displacement of the idealised curve d_e were determined by considering the equivalent input energy of the bi-linear and hysteresis envelope curves (Equivalent Energy Elastic–-Plastic (EEEP) method), with the elastic stiffness of the bi-linear curve presumed to be K_{ef}, and the ultimate displacement, d_u, obtained from the tests (at a 20% reduction in load-bearing capacity of the first loading cycles, i.e. no strength impairment considered) taken as the ultimate displacement of the bi-linear curve. In accordance with EN 12512, yield slip, d_y, was defined as the intersection of the $K_{10\text{-}40}$ secant stiffness curve and the tangent curve to hysteresis envelope with an inclination of 1/6 $K_{10\text{-}40}$. In accordance with EN 12512, ductility, μ, is defined by the dependence of yield slip (d_u/d_y). Since both d_y and d_u and consequently μ are largely dependent from the chosen idealisation criterion/criteria (large differences in ductilities calculated using different idealisation criteria were for GFB-to-timber connections with staples confirmed by Schwendner et al [27]), also a more conservative average ductility, evaluated from the elastic displacement of the bi-linear curve (d_u/d_e, denoted as $\mu(EEEP)$), is provided in Fig. 7. For the cyclic tests, average results of both directions of loading are presented.

One behaviour characteristic, which cannot be obtained from the hysteresis envelopes curves or results of monotonic tests, but only from hysteresis, is the amount of dissipated energy. The bigger the area of the

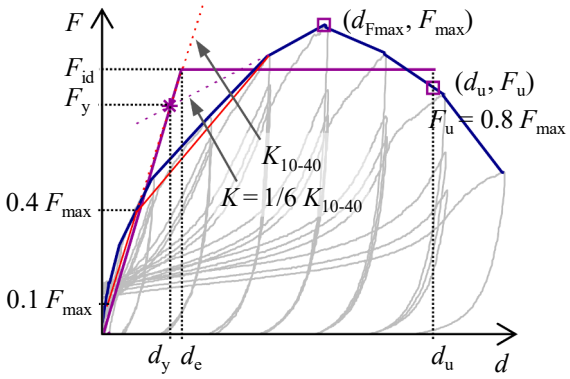

Fig. 8. Characteristic points of the envelope curve with yield point (d_y, F_y) according to EN 12512, and a bi-linear curve considering the additional equivalent energy criterion (EEEP).

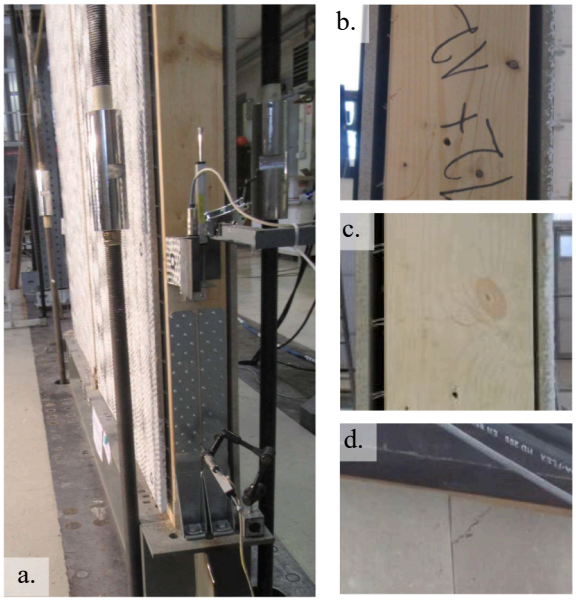

Fig. 9. Damage mechanisms of the basic panels with staples spaced 75 mm apart in one row; plastic deformations and withdrawal from the timber with post-peak failure of the staples following cyclic tests in a. Panel B16-16; b. Panel B12-12; and c. Panel B12-16; d. Typical damage to the CPB in the basic panel variations.

hysteresis loops under the curve, the higher the relative energy dissipation is in relation to the input energy. Since the dissipated energy depends on the lateral displacement loading to which the elements are subjected, energy dissipation is usually evaluated relative to the potential (input) energy. Relative energy dissipation was evaluated for all tests through the equivalent viscous damping coefficient (v_{eq}), which was calculated for each loading cycle according to EN 12512. The average results for the 3rd loading cycles $v_{eq,ave}$ (3rd), and the average minimum values $v_{eq,min}$ obtained in the B12-12 and B16-16 tests, are also presented in Fig. 7.

3.2. Tests on full-scale wall elements

The panel tests also showed a ductile failure mechanism under lateral loading, with plastic deformations and withdrawal of the staples (and CPB) from the timber frame in the basic panels with varying CPB thickness and one row of staples spaced 75 mm apart (Fig. 9a-c, respectively). Only minor damage occurred in the CPB (Fig. 9d). In some cases cracks in the corners of the CPB resulted in them falling off during the post-peak loading.

The B12-12 panels with stronger sheathing-to-timber connections also exhibited plastic deformations and withdrawal of the staples (Fig. 10a). In panels with a staple configuration of 75x2 (Fig. 10b) and 37.5x1 (Fig. 10c), however, the critical mechanism defining the lateral load-capacity of the panels was the block shear failure of the CPB along the connections. In the specimens with one row of staples (placed closer together), the CPB cracked diagonally (Fig. 10d), whereas in the specimen with two rows of staples the failure occurred across the connections, prevailingly along the inner row of staples. In some cases, significant damage of the outer stud at the hold down position also occurred (Fig. 10c). It must be noted that the failure of the CPB along the connections was not instant, but propagated with an increase in lateral load.

Overall, besides the higher lateral load-bearing capacity, which was expected, the B16-16 panels also exhibited a higher lateral deformation capacity, as is evident from Fig. 11a, where the typical lateral load – displacement hysteresis curves of the B12-12 and B16-16 panels obtained from cyclic tests are compared and the results of the monotonic tests presented. The hysteresis curves of the two stronger B12-12 variations tested clearly show that the increased number of sheathing-to-timber connections increased the lateral load-bearing capacity of the panels, as seen in Fig. 11b. The influence on the response is more evident

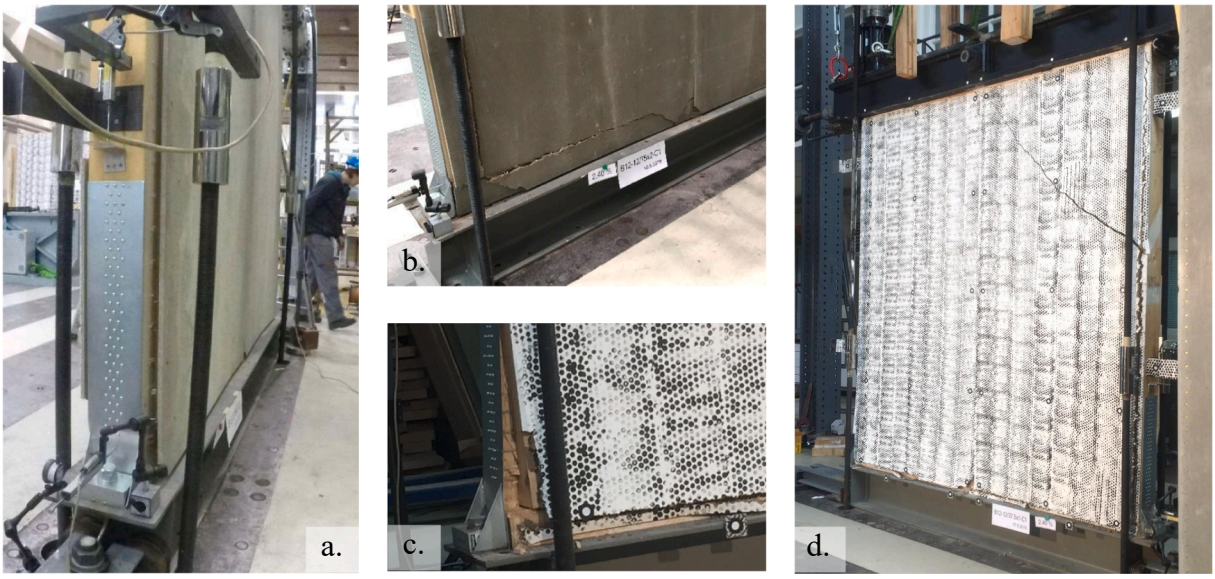

Fig. 10. a. Plastic deformations and withdrawal of staples in the B12-12/75x2 panel; b. CPB failure along the connections in the B12-12/75x2 panel; c. Failure of the CPB in the sheathing-to-timber connections of the B12-12/37.5x1 panel, with damage to the outer stud; d. Failure mechanism of the B12-12/37.5x1 panel, with a diagonal crack in the CPB.

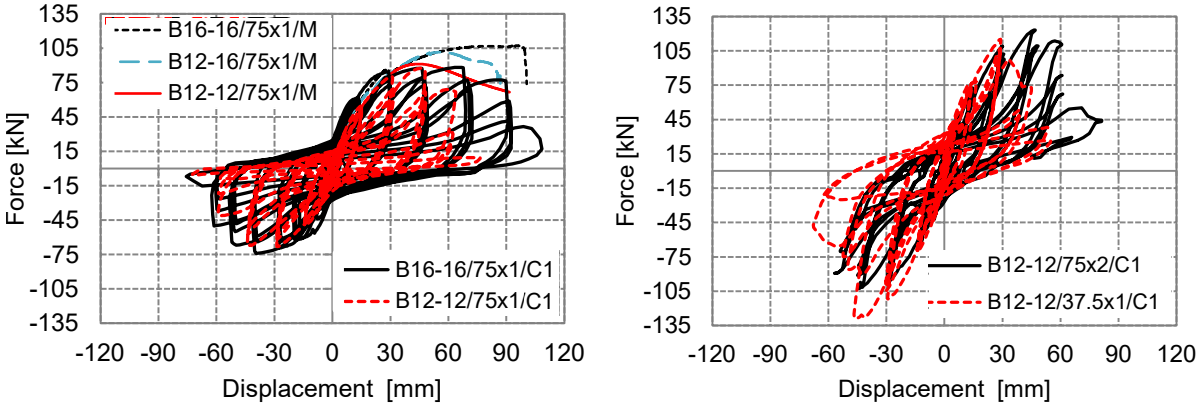

Fig. 11. Typical lateral load - lateral displacement (hysteresis and monotonic) curves obtained for the basic panels (75x1) and the stronger B12-12 panels.

in Fig. 12, where the typical hysteresis envelopes of the three loading cycles obtained in the first loading direction are presented for tests of both the basic and stronger panels. Table 3 shows the average results of all tests in both directions of loading; besides the mechanical parameters for tests of connections previously explained, the table also provides the lateral displacements of panels at 10% and 40% F_{max}, i.e. d_{10} and d_{40}, respectively, the displacement at which F_{max} was obtained, d_{Fmax}, and the ultimate drift, Δ_u, corresponding to the ultimate displacement, d_u. Furthermore, the decrease in lateral load resistance (i.e. strength impairment) in the 3rd loading cycle, for the amplitude displacement at which maximum resistance was obtained (F_{max}^{3rd}), is presented. It can at this point be mentioned that the strength impairment was also for the analysis of the panels' tests not considered in the definition of d_u. Finally, minimum and maximum values of the equivalent viscous damping are presented, evaluated for each test according to EN 12512 (labelled $\nu_{eq}^{(1-3)}$), followed by the average values of the third loading cycle ($\nu_{eq,ave}^{(3)}$) for each test.

4. Discussion

4.1. Sheathing-to-frame connections

The cyclic tests showed an average load-bearing capacity per staple, F_{max}, of 1.14 kN in the B12 connection (1.53 × 11.25 × 45 mm staples, coefficient of variation (CV) of 12%), and 1.60 kN in the B16 connection (2.0 × 11.76 × 50 mm staples, CV 11%). These values consider the average values of both loading directions; lateral load-bearing capacities in the first loading direction were 7% higher on average, while the idealised bi-linear resistances, F_{id}, were, on average, approximately 15% lower. Moreover, lateral load-bearing capacities were, on average, 25% higher in the monotonic tests than in the cyclic tests, with average values of 1.41 kN (CV 16%) and 2.0 kN (CV 15%) in the B12 and B16 connections, respectively. Slip at failure was also significantly lower in the cyclic tests compared to the monotonic tests, with values more than 65% lower, also leading to a reduction in average ductility of more than 35%.

Nevertheless, a relatively high ductility was with the favourable failure mechanism also obtained in the cyclic tests, i.e. for both types of connections the ductility, μ, was larger than 6, if the definition according to EN 12512 is considered. In the B16 connection the ductility is also higher than 6 if, in addition to EN 12512, a more conservative EEEP

criterion is considered ($\mu_{(EEEP)}$). This is emphasized because there are significant differences in the ductilities calculated from the two methods described. In the B12 connection the ductility, μ, is 20% higher when calculated using EN 12512 compared to $\mu_{(EEEP)}$, while in the B16 connection the difference is even higher, reaching 50%.

Energy dissipation, expressed relative to input energy in terms of the equivalent viscous damping coefficient, proved that energy dissipation decreased with repeating cycles but remained higher than 10% throughout all tests (average minimal values 11.2% and 11.7% for the B12 and B16 connections, respectively). A small decrease of equivalent viscous damping was obtained for the first loading cycles also with increasing amplitude displacements over 2 mm (for all amplitude displacements except cycles before failure), which can be explained by the smaller frictional forces between the boards and the timber [17]. The range of damping obtained throughout all the cycles is in accordance with the results of Sartori and Tomasi [5], who reported damping values of between 11.7% and 19.7% for both OSB-nailed and GFB-stapled connections, but lower than those seen by Verdret et al [7], who reported values of over 40% at ultimate displacement in OSB-timber stapled connections.

4.2. Seismic response of the full-scale wall panels

4.2.1. Basic panels (varying in sheathing thickness and staple size, whilst maintaining the same staple configuration)

By comparing the average results of the basic panels with varying sheathing thickness (Fig. 13), it can be seen that, in cyclic tests, the load-bearing capacity of panels with thinner CPB and weaker staples (B12-12) is reduced by only 8% in comparison to the panels with thicker CPB and stronger staples (B16-16) (if idealised resistances are compared the reduction is 10%). According to the monotonic tests this reduction is slightly higher (15%), but this is still low considering the analytical models in EC5, where estimation of the panels' resistance is linearly dependent on the load-bearing capacity of the connectors (according to the connections tests the resistance of the B12 connection was 30% lower than that of the B16).

In both cyclic and monotonic tests the lateral resistance of the asymmetrical panel B12-16 was between the resistances of the B12-12 and B16-16 panels, proving that, in the type of panels tested, using sheathing material of different thicknesses on either side of the panel does not negatively influence the resistance, as has previously been established in the literature for other panel configurations with sheathing materials of different brittleness (i.e. GFB and OSB) on either side [11]. On the other hand, the lateral deformation capacity seems to be governed by the weaker side of the panel, or may even be additionally reduced as a result of the asymmetry of the panel. In cyclic tests the deformation capacity of the B12-12 and B12-16 panels was, on average, 27% and 33% lower, respectively, than that of the B16-16 panels. Nevertheless, since a favourable failure mechanism of the B12-16 panel occurred, and the ductility according to EN 12512 was still higher than 4, a minimal 50% reduction in lateral load resistance for asymmetric panels in general, as defined by EC5, proved to be too conservative.

All three variations of the basic panels exhibited similar elastic stiffness, which decreased from the B16-16 to the B12-12 panel, except in the monotonic test of B12-16. This discrepancy can be explained by the stronger and stiffer anchorage used in this test.

For all three types of panel, the strength impairment at maximum resistance cycles was more than 20% when considering both loading directions (Table 3), but lower in the B16-16 panels, with an average of 20.6% compared to 22.6% and 24.2% in B12-16 and B12-12, respectively. Also in this regard, the asymmetry of the panel does not negatively influence the response. In the B16-16 panels maximum resistance was achieved at a higher displacement, d_{Fmax} (on average 49.9 mm) compared to in the B12-16 and B12-12 panels (40.6 mm and 36.6 mm, respectively).

Furthermore, panel B16-16 exhibited the highest energy dissipation, with an average equivalent viscous damping in the 3rd loading cycle of 22%. Lower but similar values were obtained in B12-12 and B12-16, with an average of 14.5% in both types of walls. These values are in line with study of Seim et al [6], who reported that average 3rd cycle equivalent viscous damping ranged from 12 to 20% in GFB-staple connections and 12–21% in OSB-nail connections.

It should be highlighted that the values of ductility (μ) estimated according to EN 12512 (equal to 6.92, 4.54 and 4.35 for B16-16, B12-12

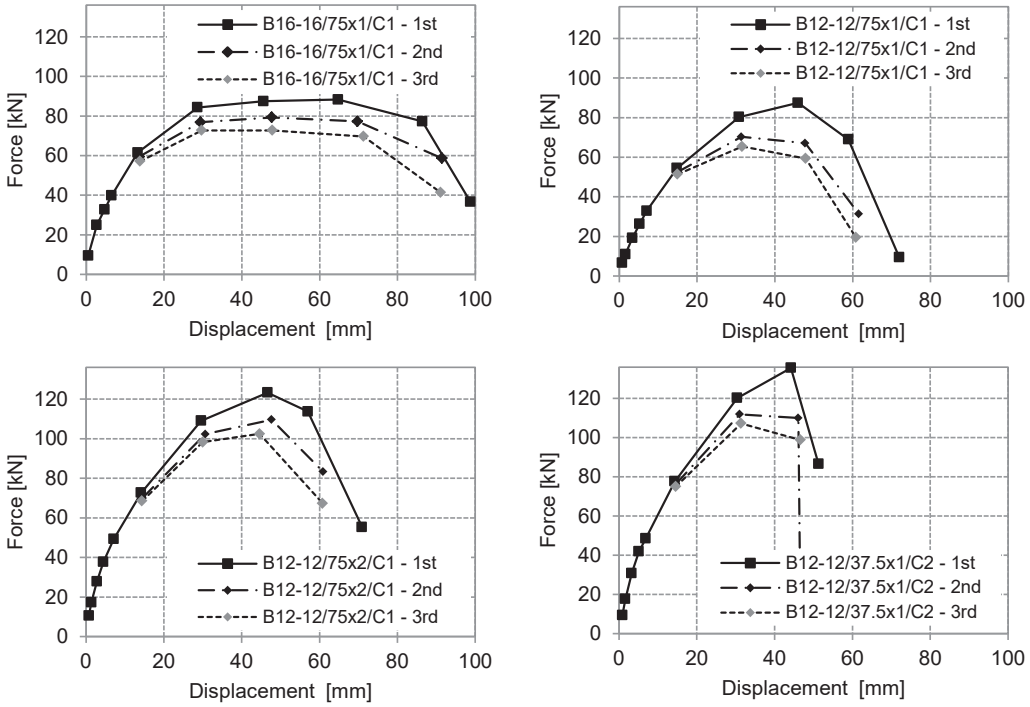

Fig. 12. Typical lateral load – lateral displacement envelopes for the 1st, 2nd and 3rd loading cycles, in the positive loading direction, for the various panels tested.

Table 3
Results of monotonic and cyclic shear tests on the wall panels.

Test	$K_{10\text{-}40}$ [kN/mm]	d_{10} [mm]	d_{40} [mm]	F_{max} [kN]	$\frac{Fmax - Fmax^{3rd}}{Fmax}$	d_{Fmax} [mm]	d_u [mm]	Δ_u [%]	ν_{eq} [/] (1–3)	$\nu_{eq,ave}$ [/] (3)	K_{ef} [kN/mm]	d_y [mm]	d_e [mm]	F_{id} [kN]	$\mu = d_u/d_y$ [/]	$\mu_{(EEEP)} = d_u/d_e$ [/]
B16-16/75x1/M	4.73	2.27	9.07	107.3	/	75.4	100.3	3.80	/	/	4.09	16.4	24.8	101.3	6.66	4.41
B12-16/75x1/M	5.44	1.87	7.46	101.5	/	55.9	85.6	3.24	/	/	4.89	11.0	19.1	93.2	9.68	5.59
B12-12/75x1/M	4.25	2.15	8.58	91.2	/	45.0	79.0	2.99	/	/	4.35	10.5	19.1	83.2	7.62	4.19
B16-16/75x1/C1	5.71	0.29	4.61	81.2	20.8%	52.1	73.2	3.03	0.19–0.44	0.22	6.40	9.7	11.7	73.9	7.53	6.18
B16-16/75x1/C2	4.80	1.05	6.37	84.6	20.4%	47.7	78.7	3.26	0.13–0.27	0.22	5.09	13.1	15.3	77.2	6.32	5.33
B12-16/75x1/C1	4.50	1.16	6.73	82.7	24.1%	44.4	66.4	2.74	0.05–0.23	0.16	4.73	13.7	15.4	72.6	4.98	4.43
B12-16/75x1/C2	5.14	0.57	5.26	80.1	21.0%	36.8	44.5	1.84	0.08–0.37	0.13	5.61	10.9	11.9	70.0	4.10	3.58
B12-12/75x1/C1	4.25	0.95	6.51	77.8	23.4%	37.4	54.4	2.25	0.12–0.25	0.15	4.53	14.1	15.5	68.9	3.96	3.62
B12-12/75x1/C2	5.17	0.58	4.97	74.2	24.9%	35.7	46.6	1.93	0.06–0.23	0.14	5.61	10.4	12.5	65.5	4.74	4.08
B12-12/75x2/C1	6.25	0.71	6.16	112.9	17.6%	45.8	59.2	2.45	0.03–0.19	0.08	6.82	12.7	14.7	99.3	4.74	4.08
B12-12/75x2/C2	7.84	0.82	5.45	118.3	19.8%	42.5	57.4	2.38	0.02–0.31	0.16	8.38	11.7	13.2	106.8	5.83	4.78
B12-12/37.5x1/C1	6.39	0.94	6.81	122.0	20.3%	37.6	42.2	1.75	0.05–0.33	0.16	6.84	14.7	15.5	103.2	2.86	2.74
B12-12/37.5x1/C2	6.56	1.05	6.82	122.7	19.9%	36.9	48.5	2.01	0.07–0.34	0.12	6.95	14.7	15.8	106.6	3.49	3.23

Note: For cyclic (C) tests, the results in the table present the average results from both directions of loading.

and B12-16, respectively; Fig. 13), are, similar to in the connections, relatively high; the ductilities $\mu_{(EEEP)}$ evaluated from the bi-linear curves, considering EN 12512 and the additional energy criterion, are, on average, 20% lower than μ. The choice of methodology is important for analysis of the results, both in terms of comparison of the results of different tests as well as to compare the results to analytical models, as can also be illustrated in the case of the lateral load-bearing capacities evaluated; monotonic tests of LFTP proved resistance was, on average, 25% higher than in the cyclic tests (considering both directions of loading), while the idealised values of cyclic tests were, on average, 10% lower than the maximal values. The idealised lateral resistance therefore provides additional safety and partially compensates for the strength impairment.

4.2.2. *Influence of the number and configuration of fasteners*

With almost twice the number of staples in the B12-12/75x2 panels, and double in B12-12/37.5x1, the lateral load-bearing capacities were significantly higher, with a 52% average increase in the first panel type and a 61% increase in the second type of panel compared to the basic B12-12/75x1 panels. This confirms the findings established in [12], which reported that lateral load-bearing capacity is not linearly dependent on the spacing of connectors. Due to the less favourable failure mechanism with diagonal failure in the B12-12/37.5x1 panels, however, the ultimate displacement capacity, d_u, and consequently also the ductility of this panel, decreased to approximately 80% d_u of the basic B12-12 panels (B12-12/75x1).

Conversely, positioning the staples in two rows in the B12-12/75x2 panels proved to increase the lateral load-bearing capacity of the panels, without compromising its deformation capacity, despite the different failure mechanism obtained; the average ultimate capacity was 5% higher and, due to the increased panel stiffness (elastic stiffness on average 50% higher), ductility was also 15% higher than in the basic panel. This is in agreement with results of numerical studies [10], where the ultimate limit displacement capacity is prevailingly dependent on the aspect ratio of the LFTP, but not influenced by the spacing of fasteners, number of studs or cross-sectional size.

The equivalent viscous damping coefficients, ν_{eq}, were similar for the B12-12 panels across all three staple configurations, with the exception of the B12-12/75x2/C1 test (Fig. 14). This partially agrees with the findings by Di Gangi et al [10], who state that the spacing distance does not influence ν_{eq}. No peculiarities in the damage mechanism in the B12-12/75x2/C1 test that could explain the evidently lower ν_{eq} were, however, observed.

4.2.3. *Comparison of the experimentally obtained lateral load-bearing capacities to the results of analytical models, according to EC5*

Connections. The lateral load-bearing capacities of the stapled connections tested (single dowel-type fastener) were evaluated according to European yield model (EYM) in EC5 for single shear panel-to-timber connections [3] with neglecting the contribution of the rope effect (Eq. (1)) where d is the fastener diameter, t_1 and t_2 the board and the timber penetration depths, respectively, $f_{h,1,k}$ and $f_{h,2,k}$ the characteristic embedment strengths in board and timber members, respectively, with $f_{h,1,k}$ assumed equal to 30 $d^{-0,3}$ $t^{0,6}$, as proposed in the EC5 for hardboards, β the ratio between the embedment strengths of the members, and $M_{y,Rk}$ the characteristic yield moment of the staple and assumed according to the code for staples with minimum tensile wire strength of 800 MPa as 240 d[mm]^{2,6}. The characteristic values obtained, $F_{f,k,EC5}$, were 0.681 kN and 1.038 kN for the B12 and B16 staple connections, respectively (Table 4, left). According to the calculation, of the six possible failure mechanisms, mechanism c), i.e. bearing failure in both members (timber and sheathing) due to embedment, is critical in both types of connections. If $M_{y,Rk}$ according to the staples' declaration of performance are assumed (620 and 1040 Nmm for staples in B12 and B16 connections, respectively), mechanism f) becomes critical for the

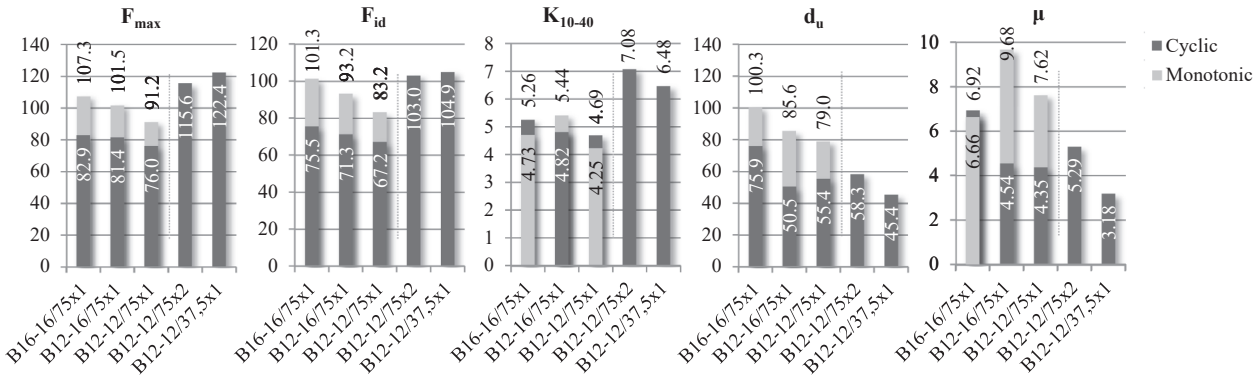

Fig. 13. Comparison of results of the various panels.

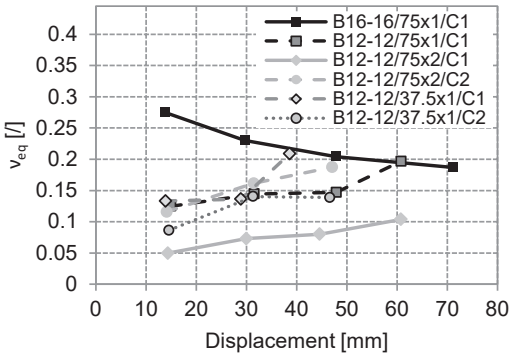

Fig. 14. Equivalent viscous damping coefficient for wall panels in 3rd loading cycle displacement steps.

Table 4
Analytical and experimental lateral load-bearing capacity of the staples (left), and the panels tested, considering various load-bearing capacities of the staples and different methods from EN 1995-1-1 for calculation of the panels' capacity (right).

Staple	Analytical		Experimental		Panel		Analytical – F_v (an.)				Experimental – F_{max} (exp.)	
							Method A		Method B			
	(Charact.*)	Mean	(Charact.*)	Mean			Considered staple load-bearing capacity				Cyclic	Monotonic
	($F_{f,k,EC5}$)	$F_{f,m,EC5}$	($F_{f,k,Exp}$)	$F_{f,m,Exp}$			$F_{f,m\ (EC5)}$	$F_{f,m\ (Exp.)}$	$F_{f,m\ (EC5)}$	$F_{f,m\ (Exp.)}$	$F_{max,C}$ ($F_{id,C}$)	$F_{max,M}$ ($F_{id,M}$)
B16	(1.04)	1.25	(1.22)	1.60	B16-16	/ 75x1	78.4	101.0	81.4	104.9	82.9 (75.5)	107.3 (101.3)
					B12-16	/ 75x1	64.9 (**32.5)	86.5 (**43.2)	56.5	76.1	81.4 (71.3)	101.5 (93.2)
B12	(0.68)	0.82	(0.90)	1.14	B12-12	/ 75x1	51.4	72.0	44.1	61.7	76.0 (67.2)	91.2 (83.2)
					B12-12	/ 75x2	91.3	127.7	88.2	117.7	115.6 (103.0)	/
					B12-12	/ 37.5x1	102.9	143.9	140.4	196.4	122.4 (104.9)	/

Note: *The characteristic analytical and experimental load-bearing capacities of staples stated in brackets are not considered for the calculation of lateral load-bearing capacities of the panels presented on the right side of the table. **In the asymmetric B12-16 panels the values presented in brackets are reduced due to the asymmetry, as outlined in EC5.

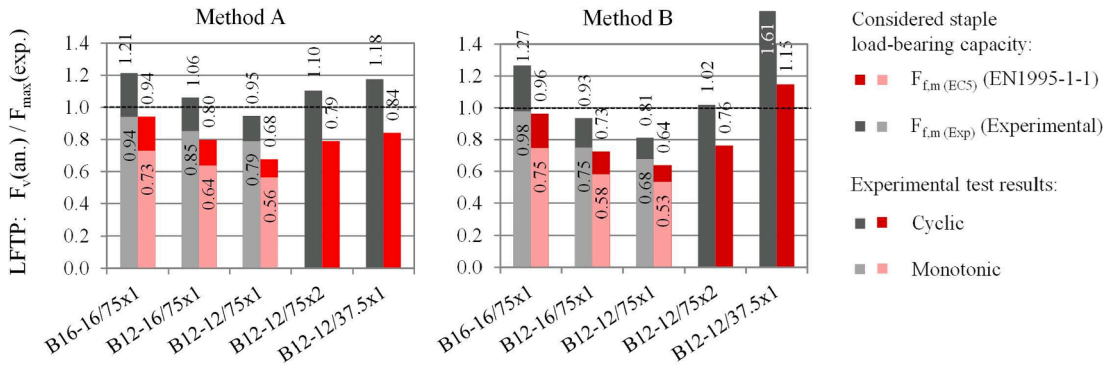

Fig. 15. Ratio of the analytically estimated load-bearing capacity of panels F_v (an.) (according to methods A and B, considering the analytical and experimental shear load-bearing capacity of the staples: $F_{f,m\,(EC5)}$ vs. $F_{f,m\,(Exp)}$) to that experimentally obtained F_{max} (exp.), in the monotonic and cyclic panel tests.

B16 connection yielding 3% lower load-bearing capacity (1.006 kN).

$$F_{f,k,EC5} = \min \begin{cases} f_{h,1,k} t_1 d & a) \\ f_{h,2,k} t_2 d & b) \\ \frac{f_{h,1,k} t_1 d}{1+\beta} \left[\sqrt{\beta + 2\beta^2 \left[1 + \frac{t_2}{t_1} + \left(\frac{t_2}{t_1} \right)^2 \right] + \beta^3 \left(\frac{t_2}{t_1} \right)^2} - \beta \left(1 + \frac{t_2}{t_1} \right) \right] & c) \\ 1.05 \frac{f_{h,1,k} t_1 d}{2+\beta} \left[\sqrt{2\beta(1+\beta) + \frac{4\beta(2+\beta) M_{y,Rk}}{f_{h,1,k} d t_1^2}} - \beta \right] & d) \\ 1.05 \frac{f_{h,1,k} t_2 d}{1+2\beta} \left[\sqrt{2\beta^2(1+\beta) + \frac{4\beta(1+2\beta) M_{y,Rk}}{f_{h,1,k} d t_2^2}} - \beta \right] & e) \\ 1.15 \sqrt{\frac{2\beta}{1+\beta}} \sqrt{2 M_{y,Rk} f_{h,1,k} d} & f) \end{cases} \tag{1}$$

$$F_{f,k,Exp} = (1 - k_n \bullet CV) F_{f,m,Exp} \tag{2}$$

From experimental tests, characteristic values of the shear load-bearing capacities, $F_{f,k,Exp}$, of a single-staple connection were calculated considering Eq. (2) from the mean results, $F_{f,m,Exp}$, following the guidelines in EN 1990 [28]. For the number of samples, n, tests, in which failure of the connection was critical, were considered, while k_n coefficient was presumed in dependence of number of samples as given in the code for the 5% characteristic fractile and a normal distribution with an unknown CV. The EN 12512 does not specify how to determine the nominal load-bearing capacity of the connection from experimental results; the characteristic experimental values, $F_{f,k,Exp}$, were therefore conservatively evaluated from the average cyclic tests results, considering both loading directions (as one test result), and were found to be equal to 0.889 kN for B12 (n, k_n and CV equal 11, 1.72 and 12.3%, respectively) and 1.221 kN for B16 (n, k_n and CV equal 6, 2.18 and 9.6%, respectively) connections. In comparison to $F_{f,k,Exp}$, the analytically determined $F_{f,k,EC5}$ (considering $M_{y,Rk}$ as 240 d[mm]^{2,6}) are underestimated by 24% and 15%, respectively. The underestimation is higher when the $F_{f,k,EC5}$ is compared to experimental results from only the first loading direction (by 30% and 18%, respectively), or to the results of the monotonic tests (by 17% and 33%, respectively, noting that a smaller number of samples (n equal 4) are considered when calculating the characteristic values from the monotonic tests compared to from the cyclic test results). On the other hand, when compared to the idealised results of cyclic tests, the estimation using EC5 is closer to experimental results; the $F_{f,k,EC5}$ underestimates the idealised cyclic tests results by 14% in the B12 connection, compared to only 6% in the B16 connection. The results of cyclic tests coincide with conclusions of Seim et al [8] for nailed OSB-to-timber connections that the capacity is according to the EYM estimated more conservatively for connections with thinner than with thicker boards.

Panels. The lateral load-bearing resistances of the panels were analytically calculated considering methods A (Eq. (3)) and B (Eq. (4)) outlined in EC5 (Sections 9.2.4.2 and 9.2.4.3), which both assume the failure of the panel to occur with ductile failure of the sheathing-to-timber connections:

$$F_v(an.) = \frac{F_{f,m} b c}{s} \tag{3}$$

$$F_v(an.) = \frac{F_{f,m} b}{s_0} k_d k_q k_s k_n \tag{4}$$

$$s_0 = \frac{9700 d}{\rho_k} \tag{5}$$

$$k_d = \frac{b}{h}, \text{for} \frac{b}{h} \le 1.0 \tag{6}$$

$$k_q = 1 + \left(0.083q - 0.0008q^2\right) \left(\frac{2.4}{b} \right)^{0.4} \tag{7}$$

$$k_s = \frac{1}{0.86 \frac{s}{s_0} + 0.57} \tag{8}$$

$$k_n = \frac{F_{v,Rd,max} + 0.5 F_{v,Rd,min}}{F_{v,Rd,max}}, \text{for sheathing on both sides,} \tag{9}$$

where $F_{f,m}$ presents the shear capacity of the sheathing-to-timber connections, b the panel length, s the distance between the sheathing-to-timber connections, c a coefficient considering panel width to height aspect ratio (for the tested panels equal 1.0), s_0 the basic fastener spacing (Eq. (5), where d is the staple diameter and ρ_k characteristic density of the timber frame), and k_d, k_q, k_s and k_n coefficients determined in dependence of dimensions (k_d, Eq. (6)), equivalent uniformly distributed vertical load q (k_q, Eq. (7)), fastener spacing (k_s, Eq. (8)) and the sheathing material (k_n, Eq. (9), where $F_{v,Rd,max}$ and $F_{v,Rd,min}$ are the design racking strengths of the stronger and weaker sheathing side of the panel, respectively).

Since, according to the methods, the lateral load-bearing capacity of staples linearly affects the load-bearing capacity of the panels, both the experimental, $F_{f,m,Exp}$, and the analytical, $F_{f,m,EC5}$, mean values for the staples lateral load-bearing capacity were considered in the analytical calculation of the panels' lateral load-bearing resistance (F_v(an.)), with $F_{f,m,EC5}$ assumed as 1.2 $F_{f,k,EC5}$. The calculated analytical load-bearing resistances of panels are presented in Table 4, together with the average maximal results from the cyclic and monotonic tests (F_{max}, denoted with subscripts C and M, respectively) and the average idealised results (additional subscript id), since the accuracy and conservativeness of the analytical estimations vary highly in dependence to which

experimental results they are compared to. Moreover, the ratios of the various analytical (Method A and B) to experimental results for the different types of panel studied are presented in Fig. 15. In both diagrams the columns depicted in red represent the ratios where the analytical results consider the staple load-bearing capacities determined analytically according to EC5, whereas those in grey consider the experimentally determined staple load-bearing capacities. The opaque columns represent the analytical results compared to the cyclic tests, while the columns with a reduced opacity apply to the monotonic tests.

It is clear that none of the methods provide good estimations for all of the panels, in which the same failure mechanism as assumed in the method was obtained (basic panels with staples spaced at a 75 mm distance). If the experimental staple load-bearing capacities are considered, both methods yield unconservative results for panels B16-16/75x1, whereas method A also for panel B12-16/75x1 (without any reduction), when compared to the maximum values obtained from the cyclic experimental tests. The lateral load-bearing capacity is underestimated also for panels B12-12/75x2 and B12-12/37.5x1, but the full lateral resistance defined through ductile failure of the sheathing-to-timber connections was for these panels in experimental tests not achieved due to CPB failure along the connections. When the basic panels' analytical results are compared to the results of the monotonic tests, however, the analytical estimation considering the actual $F_{f,m\ (Exp.)}$ are safe. Better results, in terms of a smaller error, are obtained with method A; the F_v is overestimated by 21% and underestimated by 5% in the B16-16/75x1 and B12-12/75x1 panels, respectively, compared to the cyclic test results, as oppose to Method B where the results are overestimated and underestimated by 27% and 19%, respectively.

With method A, the results are always conservative compared to the test results when the EC5 staple load-bearing capacities are considered for the calculation (even for the panels with double fasteners); underestimations of 6–32% were obtained for the various panel variations compared to the average maximal experimental test results. If analytical estimations are compared to the idealised experimental results, rather than to the maximum experimental ones, the relative error is even smaller (maximum 24% underestimation, but 4% overestimation for the B16-16 panel). As it is clear from the failure of the panels with higher number of sheathing-to-timber connections, the lateral capacity of the panel should in addition to using methods A and B be evaluated also by considering shear failure of the sheathing. If the capacity through board shear failure is estimated according to DIN 1052:2008–12 [29] ($F_v = k_v f_{v,m} t b$, where k_v is equal to 0.5 as assumed for panels with boards on both sides, $f_{v,m}$ mean shear strength of the board, considered as $1.2 f_{v,k}$, and t and b thickness and length of the panel, respectively), the lateral load-bearing capacities obtained for the panels with 12 mm and 16 mm thick boards are 117.0 and 156.0 kN, respectively. The estimations are smaller than the ones according to methods A and B for the "stronger" B12-12 panels and correspond well to experimental results; the lateral load-bearing capacity is underestimated by 1.2% for the B12-12/75x2 panels and overestimated by 4.6% for the B12-12/37.5x1 panels.

5. Conclusions

An extensive experimental campaign was conducted to evaluate and improve the seismic behaviour of shear light-frame timber panels (LFTP) using cement-particle boards (CPB) as a sheathing material. Experimental tests conducted on small specimens to study the CPB-to-timber staple connections were followed by in-plane shear tests of full-size panels. The conclusions that can be drawn from the study are as follows:

- Under cyclic loading CPB-to-timber connections with metal staples spaced 75 mm apart enable a ductile failure mechanism, with plastic deformations and withdrawal of the staples obtained for CPB of both 12 mm (B12) and 16 mm (B16) thickness. The same failure mechanism also occurred in specimens where staples were placed closer together (at spacing distances of 50 mm and 37.5 mm).
- No systematic differences were found in the load-bearing capacity of the staple connections by decreasing the spacing between staples. The characteristic values calculated from maximum load-bearing capacities obtained from cyclic tests were, however, 30% higher than that estimated according to the EC5 code provision (EYM) in the case of the B12 connection, and 18% higher in the case of the B16 connection. The results confirm the findings of Seim et al [8] that the estimated lateral load-bearing capacity of connections with thinner boards is more conservative than with thicker boards.
- The full-size basic panels with a spacing distance between staples of 75 mm, and different CPB thickness, all exhibited the ductile failure mechanism (ductility according to EN 12512 was larger than 4 in all samples), once again with deformations and withdrawal of the staples, but only slight damage to the CPB, in the corners. The lateral load-bearing capacity of the panels increased with a greater CPB thickness and the corresponding increase in staple diameter, but the increase was not linear with regard to the increase in staple load-bearing capacity, which is an assumption in the models adopted in EC5 (methods A and B).
- The asymmetry of the panel, resulting from the variation in thickness of the CPB and staples, did not have a negative influence on its lateral load-bearing capacity response, whereas the deformation capacity was found to be governed by the weaker side of the panel, and was slightly reduced compared to the symmetric panel.
- Increasing the number of staples, either by reducing the staple distance or by fastening the CPB with two rows of staples, proved to significantly increase the panels' load-bearing capacity (by more than 50%), but again not proportionally with the decrease in staple distance due to failure of the panel being controlled by the failure of the CPB. For panels with staples in two rows, CPB subsequently cracked along the connections, while a diagonal tensile failure of the CPB occurred in the panels with staples 37.5 mm apart. Consequently, the deformation capacity and ductility of the latter were lower. In the case of the former, ductility increased compared to the basic panel, since the ultimate deformation capacity obtained was similar, but stiffness increased by 50%.
- A reduction in the spacing of staples appears not to influence the relative energy dissipation of the panels tested. Similar findings were seen in the panels with varying CPB thickness.
- Both method A and B in EC5 provide non-conservative analytical predictions of the lateral load-bearing capacity for some of the basic panels tested for which ductile failure mechanism was obtained, assuming that the experimentally obtained load-bearing capacities of staple connections are used, and that the analytical results are compared to the cyclic test results (in both directions of loading). Method A provides better results in terms of smaller error, though; it overestimates the lateral load-bearing capacity of the panels with 16 mm thick CPB on both sides by 21% and underestimates the capacity of the panels with 12 mm thick CPB by 6%. Method B overestimates and underestimates the capacity of the same panels by 27% and 19%, respectively. For all basic panels, the estimations are however conservative if compared to monotonic test results. On average, the load-bearing capacity of any given panel was 25% lower in the cyclic tests compared to the monotonic tests.
- On the other hand, by assuming the load-bearing capacity of staples evaluated according to EC5, the analytical lateral load-bearing capacities of all basic panels are conservative if compared to maximal cyclic test results. They are underestimated by up to 32% with

method A, and by up to 36% with method B, with the most conservative estimations obtained for the basic panel with 12 mm thick CPB.
- In addition to methods A and B, shear failure of the sheathing boards should in design be considered for determining the lateral load-bearing capacity of the panels. A good correspondence of the panels' lateral load-bearing capacities to experimental results was for the panels, where this type of failure has indeed occurred (higher number of sheathing-to-timber connections), obtained by considering the board shear failure criterion provided in DIN 1052:2008–12. A 1.2% overestimation was obtained for panels with staples in two rows, 75 mm apart, and a 4.6% underestimation for panels with staples in one row, 37.5 mm apart.

Results of the tests conducted prove that the ductile failure mechanism, with plastic deformations of the staples in the sheathing-to-timber connections, occurs in light-frame-timber panels with CPB as a sheathing material. Furthermore, in the case of a higher seismic demand, such panels can be improved to achieve a higher lateral load-bearing capacity without decreasing the deformation capacity. In the future these tests will serve to analyse the non-linear response of buildings constructed with the panels investigated, and evaluate the behaviour factor.

Ethical approval

The authors declare that there are no issues concerning ethical standards.

Informed consent

Informed consent was obtained from all individual participants included in the study.

CRediT authorship contribution statement

Meta Kržan: Methodology, Investigation, Formal analysis, Visualization, Writing – original draft, Writing – review & editing. **Tomaž Pazlar:** Conceptualization, Methodology, Writing – original draft, Writing – review & editing, Supervision. **Boštjan Ber:** Conceptualization, Methodology, Writing – original draft, Writing – review & editing, Supervision.

Declaration of Competing Interest

The authors declare that they have no known competing financial interests or personal relationships that could have appeared to influence the work reported in this paper.

Acknowledgements

The research presented was funded through Project "Raziskovalci-2.1-ZAG-952045" (Grant No. C3330-19-952045) and "TIGR4smart" (Grant No. C3330-16-529003), both co-financed by the Republic of Slovenia, Ministry of Education, Science and Sport, and the European Regional Development Fund through the EU Cohesion Policy 2014-2020. The Slovenian Research Agency (Research Core Funding No. P2-0273) is gratefully acknowledged for funding the second author, as well as the company Rotho Blaas for donating the hold-downs for the stronger panels. The authors express great appreciation to Ivan Grašič and Jelovica hiše d.o.o. for their support in optimizing the details and construction of the panels.

References

[1] Casagrande D, Rossi S, Sartori T, Tomasi R. Proposal of an analytical procedure and a simplified numerical model for elastic response of single-storey timber shear-walls. Constr Build Mater 2016;102:1101–12. https://doi.org/10.1016/j.conbuildmat.2014.12.114.
[2] Vogrinec K, Premrov M. Influence of the design approach on the behaviour of timber-frame panel buildings under horizontal forces. Eng Struct 2018;175:1–12. https://doi.org/10.1016/j.engstruct.2018.08.014.
[3] EN 1995-1-1:2004: Eurocode 5: Design of timber structures - Part 1-1: General - Common rules and rules for buildings. CEN; 2004.
[4] Fonseca FS, Rose SK, Campbell SH. Nail, wood screw, and staple fastener connections. CA: CUREE Richmond; 2002.
[5] Sartori T, Tomasi R. Experimental investigation on sheathing-to-framing connections in wood shear walls. Eng Struct 2013;56:2197–205. https://doi.org/10.1016/j.engstruct.2013.08.039.
[6] Seim W, Kramar M, Pazlar T, Vogt T. OSB and GFB As Sheathing Materials for Timber-Framed Shear Walls: Comparative Study of Seismic Resistance. J Struct Eng 2016;142:E4015004. https://doi.org/10.1061/(ASCE)ST.1943-541X.0001293.
[7] Verdret Y, Faye C, Elachachi SM, Le Magorou L, Garcia P. Experimental investigation on stapled and nailed connections in light timber frame walls. Constr Build Mater 2015;91:260–73. https://doi.org/10.1016/j.conbuildmat.2015.05.052.
[8] Seim W, Schick M, Waschkowitz T. The European Yield Model (EYM) for laterally loaded timber connections with smooth nails. Wood Mater Sci Eng 2021:1–14. https://doi.org/10.1080/17480272.2021.1983870.
[9] van de Lindt JW. Evolution of Wood Shear Wall Testing, Modeling, and Reliability Analysis: Bibliography. Pract Period Struct Des Constr 2004;9(1):44–53. https://doi.org/10.1061/(ASCE)1084-0680(2004)9:1(44).
[10] Di Gangi G, Demartino C, Quaranta G, Monti G. Dissipation in sheathing-to-framing connections of light-frame timber shear walls under seismic loads. Eng Struct 2020;208:110246. https://doi.org/10.1016/j.engstruct.2020.110246.
[11] Sartori T, Piazza M, Tomasi R, Grossi P. Characterization of the mechanical behaviour of light-frame timber shear walls through full-scale tests. World Conf Timber Eng 2012 WCTE 2012;2012(3):8.
[12] Bagheri MM, Doudak G. Structural characteristics of light-frame wood shear walls with various construction detailing. Eng Struct 2020;205:110093. https://doi.org/10.1016/j.engstruct.2019.110093.
[13] Dobrila P, Premrov M. Reinforcing methods for composite timber frame–fiberboard wall panels. Eng Struct 2003;25(11):1369–76. https://doi.org/10.1016/S0141-0296(03)00109-3.
[14] Sadeghi Marzaleh A, Nerbano S, Sebastiani Croce A, Steiger R. OSB sheathed light-frame timber shear walls with strong anchorage subjected to vertical load, bending moment, and monotonic lateral load. Eng Struct 2018;173:787–99. https://doi.org/10.1016/j.engstruct.2018.05.044.
[15] Dujic B, Aicher S, Zarnic R. Testing of wooden wall panels applying realistic boundary conditions. In: 9th World Conference on Timber Engineering 2006 (WCTE 2006), Portland, Oregon, USA; 2006.
[16] Jayamon JR, Line P, Charney FA. State-of-the-Art Review on Damping in Wood-Frame Shear Wall Structures. J Struct Eng 2018;144(12):03118003. https://doi.org/10.1061/(ASCE)ST.1943-541X.0002212.
[17] Steiger R, Fink G, Nerbano S, Hack E, Beyer K. Experimental investigation of friction stresses between adjacent panels made of Oriented Strand Board (OSB) and between OSB panels and glued laminated timber (GLT) frame members. Mater Struct 2017;51:2. https://doi.org/10.1617/s11527-017-1124-5.
[18] DIBt. ETA-16/0535: haubold staples d = 1,53 - 1,80 - 2,00 mm fasteners for timber constructions for long term or permanent load duration withdrawal capacity. 2019.
[19] ISO 16670:2003 Timber structures - Joints made with mechanical fasteners - Quasi-static reversed-cyclic test method n.d. ISO; 2003.
[20] OiB. ETA-12/0373 of 03.11.2017: Schmid screws RAPID®, STARDRIVE and SP. 2017.
[21] ETA-Danmark. ETA-06/0106 of 2018/12/18: Three-dimensional nailing plate (timber-to-timber/timber-toconcrete angle bracket). 2018.
[22] Schick M, Seim W. Overstrength values for light frame timber wall elements based on reliability methods. Eng Struct 2019;185:230–42. https://doi.org/10.1016/j.engstruct.2019.01.034.
[23] ETA-Danmark. ETA-11/0086 of 26/01/2015: Three-dimensional nailing plate (Angle brackets and hold-downs for timber-to-timber or timber-to-concrete or steel connections). 2015.
[24] ETA-Danmark. ETA-07/0285 of 2018/06/12: Three-dimensional nailing plate (timber to timber and timber to concrete/steel hold downs and post bases). 2018.
[25] SIST EN 594:2011 Timber Structures - Test methods - Racking strength and stiffness of timber frame wall panels. SIST; 2011.
[26] EN 12512:2005. Timber structures - Test methods - Cyclic testing of joints made with mechanical fasteners. CEN; 2005.
[27] Schwendner S, Seim W, Hummel J. Light-frame walls with OSB and GFB sheathing under impact - a comparative study. In: 2018 World Conference on Timber Engineering (WCTE 2018), Seoul, Republic of Korea; 2018.
[28] EN 1990: 2002: Eurocode - Basis of structural design. CEN; 2002.
[29] DIN 1052:2008-12. Entwurf, Berechnung und Bemessung von Holzbauwerken - Allgemeine Bemessungsregeln und Bemessungsregeln für den Hochbau. DIN; 2008.